Water Research 183 (2020) 116110

Contents lists available at ScienceDirect

Water Research

journal homepage: www.elsevier.com/locate/watres

High-efficient microbial immobilization of solved U(VI) by the *Stenotrophomonas* strain Br8

Iván Sánchez-Castro [a, *], Pablo Martínez-Rodríguez [a], Fadwa Jroundi [a], Pier Lorenzo Solari [b], Michael Descostes [c], Mohamed Larbi Merroun [a]

[a] Department of Microbiology, University of Granada, Campus Fuentenueva s/n, 18071, Granada, Spain
[b] Synchrotron SOLEIL, MARS beamline, L'Orme des Merisiers, Saint-Aubin BP 48, 91192, Gif-sur-Yvette Cedex, France
[c] R&D Department, Orano Mining, Chatillon, 92330, France

ARTICLE INFO

Article history:
Received 6 March 2020
Received in revised form
23 June 2020
Accepted 24 June 2020
Available online 1 July 2020

Keywords:
Porewaters
Bioremediation
Biomineralization
Uranium
EXAFS
Bacteria

ABSTRACT

The environmental impact of uranium released during nuclear power production and related mining activity is an issue of great concern. Innovative environmental-friendly water remediation strategies, like those based on U biomineralization through phosphatase activity, are desirable. Here, we report the great U biomineralization potential of *Stenotrophomonas* sp. Br8 CECT 9810 over a wide range of physico-chemical and biological conditions. Br8 cells exhibited high phosphatase activity which mediated the release of orthophosphate in the presence of glycerol-2-phosphate around pH 6.3. Mobile uranyl ions were bioprecipitated as needle-like fibrils at the cell surface and in the extracellular space, as observed by Scanning Transmission Electron Microscopy (STEM). Extended X-Ray Absorption Fine Structure (EXAFS) and X-Ray Diffraction (XRD) analyses showed the local structure of biogenic U precipitates to be similar to that of meta-autunite. In addition to the active U phosphate biomineralization process, the cells interact with this radionuclide through passive biosorption, removing up to 373 mg of U per g of bacterial dry biomass. The high U biomineralization capacity of the studied strain was also observed under different conditions of pH, temperature, etc. Results presented in this work will help to design efficient U bioremediation strategies for real polluted waters.

1. Introduction

Uranium (U) is intensively exploited and widely used for nuclear power production. Radioactive wastes generated during these operations, including spent nuclear fuel, may lead to the release of U to adjacent soils and groundwater (Gavrilescu et al., 2009) provoking deleterious side effects that are a major environmental concern. Both the mobility and the solubility of released U in nature are known to be governed by its oxidation state and chemical speciation, which in turn are controlled by biotic and abiotic processes (Suzuki and Banfield, 1999). Main primary U oxidation states are U(IV), stable as uraninite (UO_2) in anaerobic conditions, and U(VI), dominating in oxidizing conditions as the extremely soluble and stable linear uranyl ion (UO_2^{2+}) (Langmuir, 1978). The solid mineral uraninite is very sensitive to dissolved O_2 exposition which oxidizes this compound to more mobile U(VI) forms like uranyl ion. In addition, the chemical speciation of U(VI) in natural systems is highly dependent on pH. Under acidic conditions, U(VI) is likely to be adsorbed by mineral surfaces, complexed by organic matter or precipitated, forming insoluble phosphate minerals as autunite ($Ca(UO_2)_2(PO_4)_2$) (Kolhe et al., 2018). However, alkaline conditions may favor the formation of soluble uranyl compounds, such as carbonate complexes (Hsi and Langmuir, 1985; Waite et al., 1994), potentially mobile in aqueous systems. In this sense, it is well known that toxicity of uranium depends mainly on its oxidation state (U(VI)/U(IV)), being the most systemic toxicants those compounds showing highest solubility (mainly U(VI) forms like uranyl complexes). In the case of low-solubility compounds (mainly U(IV) species as uraninite, UO_2), they present low environmental and human health toxicity. The US Environmental Protection Agency and the World Health Organization have set the maximum uranium

Abbreviations: U, Uranium; STEM-HAADF, Scanning Transmission Electron Microscopy with High-Angle Annular Dark-Field; EXAFS, Extended X-Ray Absorption Fine Structure; XRD, X-Ray Diffraction; G2P, Glycerol-2-phosphate; P-ase, Phosphatase.

* Corresponding author.
E-mail address: ivansanchezcastro@gmail.com (I. Sánchez-Castro).

https://doi.org/10.1016/j.watres.2020.116110
0043-1354/

concentration level in drinking water at 30 μg/L, classifying this radionuclide as a human carcinogen (Group A).

Application of sustainable management programs, including well-designed, -operated, and -remediated mining operations, is deemed necessary to minimize U-linked environmental impacts. The inherent complexity of subsurface environments, due to changing redox conditions and diverse biogeochemical processes occurring underground, makes it essential to search for innovative remediation approaches. Standard pump-and-treat and excavation-and-removal remediation approaches are costly and inefficient in extensive areas co-contaminated with radionuclides and heavy metals. Among alternative strategies, those based on microbial processes promoting U precipitation are considered environmentally friendly, cost-effective and highly efficient (Acharya, 2015), and are therefore gaining attention in recent years.

Previous evaluation of the effects and consequences of these microbe-U interactions comes to confirm the capacity of indigenous bacteria to mediate U immobilization and thereby reduce its toxicity, suggesting applicability for bioremediation purposes (reviewed in Kolhe et al., 2018, and Merroun and Selenska-Pobell, 2008). In this context, the two microbial processes most investigated thus far are the enzymatically-catalyzed reductive precipitation of U(VI) to U(IV) and the bioprecipitation of U(VI) with ligands such as inorganic phosphates. First proposed by Lovley et al. (1991), the strategies based on U(VI) enzymatic reduction, performed by dissimilatory metal-reducing bacteria and sulfate-reducing bacteria, have been successfully applied on several occasions under laboratory conditions (Lovley and Phillips, 1992; Lovley, 2001; Xie et al., 2018) as well as at field scale in Oak Ridge site (USA) where U concentration was up to 10–60 mg/L (Wu et al., 2006, 2007). This approach entails some limitations, however, including the poor stability of bio-reduced U in the presence of oxidizing agents like O_2 or compounds such as nitrates or bicarbonates, along with Fe or Mn species (Wan et al., 2005, 2008; Wu et al., 2010; Spycher et al., 2011; Watson et al., 2013). The high solubility of resulting uraninite nanoparticles as well as other U(IV)-bearing colloids has also been reported (Bargar et al., 2008; Wang et al., 2013; Schindler et al., 2017; Neill et al., 2018).

Overall, recent research interests have switched to a second approach based on U biomineralization by aerobic or facultative bacteria exhibiting phosphatase (P-ase) enzymatic activity. Phosphohydrolases (EC 3.1.3), also known as phosphatases, are broadly categorized as acid or alkaline phosphatases, based on the pH required for their optimum activity. They are either released outside the plasma membrane or embedded as membrane components. Since free orthophosphate is rarely found in certain environments, the main role of phosphatases is supporting microbial nutrition by releasing assimilable orthophosphates from organic sources, which should be amended in case they are not naturally present. These inorganic phosphates may also act as ligands in the presence of cations, such as uranyl ion (UO_2^{2+}), inducing the bioprecipitation of U(VI) as a protective strategy for bacteria. This mechanism is the basis of promising research efforts, aiming at U precipitation by applying members of various genera like *Citrobacter*, *Pseudomonas*, *Bacillus*, *Pelosinus*, *Sphingomonas* or *Rahnella*, over a wide pH range and under aerobic and anaerobic conditions (Beazley et al., 2011; Merroun et al., 2011; Newsome et al., 2015; Bader et al., 2017; Shen et al., 2018; Kong et al., 2020). The formation of low solubility U-containing minerals like $(H_3O)_2(UO_2)_2(PO_4)_2{\cdot}6H_2O$ (Yong and Macaskie, 1995), $(NH_4)(UO_2)(PO_4){\cdot}3H_2O$ (Wall and Krumholz, 2006) and $Ca(UO_2)_2(PO_4)_2{\cdot}xH_2O$ (Mehta et al., 2013; Krawczyk-Bärsch et al., 2018), stable across a wide range of redox and pH conditions, makes this remediation alternative even more attractive.

The current work emerges as the result of a multi-criteria screening process where a significant number of bacterial isolates, recovered from rarely studied uranium mill tailing porewaters, were thoroughly analyzed at different levels (results partially published in Sánchez-Castro et al., 2017a). After the screening pipeline applied, which included molecular analyses (16S rDNA taxonomic identification), physiological tests (metals/metalloid tolerance) and microscopic observations (Scanning Transmission Electron Microscopy with High-Angle Annular Dark-Field, STEM-HAADF; Energy Dispersive X-Ray, EDX, element-distribution maps), the bacterial strain Br8 was found to be the most promising candidate. A series of assays were conducted to explore the P-ase-based U immobilization in the presence of Br8 and an organophosphate compound. Characterization of the chemical nature and localization of the U precipitates formed during biomineralization were also addressed through microscopic techniques such as STEM-HAADF and spectroscopic measurements through Extended X-Ray Absorption Fine Structure (EXAFS) spectroscopy and X-Ray Diffraction (XRD). Moreover, a thorough experimental design was developed to evaluate the influence of several parameters (time, temperature, pH and biomass concentration) on the performance of the Br8-mediated U removal process. These results are expected to provide key information for understanding the U biogeochemical cycle in subsurface environment as well as to determine the optimal conditions for the future application of this innovative strategy, under oxidizing conditions in real polluted waters, by immobilizing Br8 bacterial cells.

2. Materials and methods

2.1. Bacterial strain isolation and molecular identification

The bacterial strain used in this work (*Stenotrophomonas* sp. Br8 CECT 9810; 16S rRNA accession number HG798865) was previously isolated from U mill tailing porewaters and identified by 16S rDNA phylogeny, as described by Sánchez-Castro et al. (2017a). Physicochemical characterization of this water sample is published in Sánchez-Castro et al. (2017a).

2.2. Determination of metals' Minimum Inhibitory Concentration for bacterial growth

Filtered-sterilized stock solutions (0.1 M) of $UO_2(NO_3)_2{\cdot}6H_2O$, $Cr(NO_3)_3{\cdot}9H_2O$, $Pb(NO_3)_2$, $LaN_3O_9{\cdot}6H_2O$, $Cd(NO_3)_2{\cdot}4H_2O$, $Ni(NO_3)_2{\cdot}6H_2O$, $ZnSO_4{\cdot}7H_2O$, $Na_2MoO_4{\cdot}2H_2O$, $VOSO_4$, Eu_2O_3, and $Cu(NO_3)_2{\cdot}3H_2O$ were prepared by dissolving appropriate quantities of these metal salts in 0.1 M $NaClO_4$. In the case of Ag and Se, 1-M stock solutions of $AgNO_3$ and Na_2SeO_3 were prepared by dissolving the appropriate quantity in distilled water. To evaluate the tolerance of strain Br8 to these metals, the Minimum Inhibitory Concentration (MIC) method was applied as previously described (Sánchez-Castro et al., 2017a). This standard method is used to determine the tolerance level of a bacterium in the presence of heavy metals or other constraining agents.

2.3. Uranium immobilization assay

The ability of Br8 cells to immobilize U was studied by monitoring the removal of dissolved U(VI) as a function of U concentration in an incubation medium containing an organic phosphate source (glycerol-2-phosphate, G2P). For this purpose, MOPS-buffered (20 mM) distilled water was added to acid-washed glass Erlenmeyer flasks. Br8 cells were grown in LB broth (rich-nutrient medium; Scharlau Chemie SA, Barcelona, Spain) at 28 °C and 160 rpm for 20–24 h. Subsequently, mid-exponential growth phase

cells were washed twice with 0.9% NaCl solution and inoculated, when applicable, to a final concentration of 0.5 mg dry Br8 biomass per mL of medium (equivalent optical density at 600 nm [OD600], ≈0.5). Four U(VI) concentrations (0.01, 0.1, 0.5 and 1 mM), provided as uranyl nitrate, and/or 5 mM G2P (Sigma Aldrich), as the sole organic phosphates source, were tested. Initial pH was 6.3 in all cases and potential changes were determined by measuring the pH at the end of each assay. Flasks including no-uranium, heat-killed bacterial cells, and no-bacteria were assayed as controls. For the heat-killed cell control, the recovered Br8 biomass was exposed to 80 °C pre-incubation for 1h. Incubation of all samples was conducted at 28 °C for 48 h and under continuous shaking (165 rpm).

Once incubations were completed, aliquots from all replicate liquid samples were centrifuged at 10,000 g for 10 min at 4 °C. The supernatants and solid pellets were analyzed separately by using different techniques described below. Solid phase precipitates recovered were washed twice with 0.9% NaCl to remove the interfering elements of the incubating solution.

2.4. Quantification of phosphatase enzymatic activity

Determination of the activity of P-ase enzyme (EC 3.1.3) was based on the procedure of German et al. (2011) using the substrate 4-MUB (methylumbelliferone)-phosphate. MUB standards (0.16 μM, 0.625 μM, 1.25 μM and 2.5 μM) dissolved in Na-perchlorate buffer (pH 5) and cell suspensions were used to calculate the emission and quench coefficients for each sample using an automatic fluorometer NanoQuant equipment (TECAN, Mannedorf, Switzerland). Enzyme activity was calculated following German et al. (2011). P-ase activity was expressed as μmoles of inorganic phosphates released per hour and gram of substrate.

2.5. Determination of inorganic phosphates released

In order to calculate the inorganic phosphates concentration in solution after the incubation period, the "ammonium-molybdate method" (Murphy and Riley, 1962) based on colorimetric measurements was employed. This technique is based on the reaction of orthophosphate ions with ammonium-molybdate in acidic solution, forming phosphomolybdic acid. This compound produces an intensely blue complex upon reduction with ascorbic acid. Antimony potassium tartrate is added to increase the rate of reduction.

2.6. Quantification of uranium removal

The final concentration of U(VI) remaining in solution was determined by inductively-coupled plasma mass spectrometry (ICP-MS) with a NexION 300d (PerkinElmer) system after HNO_3 acidification using multi-element standard solutions for calibration. The concentration of U removed from solution by the cells was calculated as the difference between the initial and final U concentrations.

2.7. Cellular localization of uranium precipitates: STEM-HAADF and HRTEM/EDX analysis

Cells exposed to uranium for 48 h were harvested by centrifugation, washed twice with 0.9% NaCl and Na-cacodylate buffer (pH 7.2), fixed with glutaraldehyde in cacodylate buffer (4%) and stained with osmium tetraoxide (1%, 1 h) in the same buffer before being dehydrated through graded alcohol followed by propylene oxide treatment, and finally were embedded in epoxy resin. Ultrathin sections (0.1 μm) of the samples, obtained using an ultramicrotome, were loaded in a carbon coated copper grid and analyzed by STEM-HAADF, conducted using a FEI TITAN G2 80–300. The TEM specimen holders were cleaned by plasma prior to STEM analysis to minimize contamination. The high resolution STEM is equipped with a HAADF detector and EDX energy dispersive X-ray detector, thus providing elemental information via the analysis of X-ray emissions caused by a high-energy electron beam.

2.8. Characterization of uranium solid phase precipitated by the cells

In order to characterize the uranium solid phases precipitated during assays, EXAFS spectroscopy and XRD were applied.

2.8.1. Extended X-Ray Absorption Fine Structure (EXAFS) spectroscopy

EXAFS analyses were performed in the SOLEIL synchrotron (Paris, France). This facility is a medium energy third-generation synchrotron optimized for the production of vacuum-ultraviolet (VUV) and soft X-ray light, and operated with electrons at energy of 2.75 GeV. In particular, the measurements were performed on the MARS beamline which is dedicated to the study of radioactive samples (Sitaud et al., 2012). The beamline was built on a 1.71 T bending magnet port of the SOLEIL storage ring and operates in the hard X-ray regime from 3.5 to 35 keV with a critical energy of 8.6 keV.

EXAFS samples were prepared as previously described in Merroun et al. (2005). After incubation, cells were harvested and washed with 0.1 M $NaClO_4$, pH 7. Briefly, the pellets were dried in an oven at 30 °C for 24 h and subsequently powdered. Data were collected in fluorescence mode using a 13-element Ge detector (EG & G ORTEC, USA) and processed using the ATHENA code (Ravel and Newville, 2005). FEFF is an automated program for ab initio multiple scattering calculations of EXAFS, X-ray Absorption Near-Edge Structure (XANES) and various other spectra for clusters of atoms. Background removal was performed by means of a pre-edge linear function. Atomic absorption was simulated with a square-spline function. The theoretical phase and amplitude functions used in data analysis were calculated with FEFF8 (Ankudinov et al., 1998) using the crystal structure of meta-autunite, Ca(UO2)2(PO4)2·6H2O (Makarov and Ivanov, 1960) as a model. All fits were performed with the ARTEMIS code (Ravel and Newville, 2005). They included the four-legged multiple scattering (MS) path of the uranyl group, U-Oax-U-Oax. The coordination number (N) of this MS path was linked to N of the single-scattering (SS) path U-Oax. The radial distance (R) and Debye-Waller factor (σ2) of the MS path were respectively linked at twice the R and σ2 of the SS path U-Oax (Hudson et al., 1996). During the fitting procedure, N of the U-Oax SS path was held constant at two. The amplitude reduction factor (S02) was held constant at 1.0 for the FEFF8 calculation and EXAFS fits. The shift in threshold energy, ΔE0, was varied as a global parameter in the fits.

2.8.2. X-Ray Diffraction

For XRD analyses, U treated cells of Br8 were dried in an oven at 70 °C for 6 h. The dried pellet was scraped and crushed into a fine powder that was analyzed using a X'Pert PRO (PANalytical B·V.) equipped with Cu-Kα radiation; Ni filter; 45 kV voltage; 40 mA intensity; exploration range of 3°–60° 2θ; and goniometer speed of 0.05° 2θ s^{-1}. Previously, samples were thoroughly homogenized and crushed with an agate mortar and pestle. Patterns obtained were analyzed with XPowder software.

2.9. Effect of physicochemical and biological parameters in U biomineralization

Additional assays modifying certain experimental parameters were performed to ascertain the most favorable conditions for P-

ase activity and subsequent U removal. Time-dependent experiments considered different sampling points (0, 10 min, 30 min, 1 h, 3 h, 7 h, 24 h, 48 h and 72 h) in order to study the kinetics of the U immobilization process. The effects of different physicochemical and biological parameters including temperature (15 °C and 37 °C), pH (5 and 8) and biomass concentration (0.25 and 1 mg dry Br8 biomass per mL) were investigated to determine optimal U removal conditions. With the exception of the tested parameter and U concentration (0.1, 0.5 and 1 mM in pH tests and 0.5 mM for the rest), the experimental conditions were maintained as stated above (5 mM G2P; pH 6.3; incubation at 28 °C, 48 h, 165 rpm).

2.10. Statistical analysis and thermodynamic modeling

Data in this manuscript are presented as averages and standard deviations for three replicates per experimental condition tested. All statistical analyses were carried out using Microsoft OfficeExcel 2010. Aqueous U speciation under GC1 or GC2 was determined using Visual MINTEQ version 3.1 (http://vminteq.lwr.kth.se/download/) (VanEngelen et al., 2010).

3. Results and discussion

3.1. Br8 bacterial strain identification and heavy metal tolerance studies

Based on 16S rRNA gene analysis, the bacterial strain Br8 was found to be affiliated to the genus *Stenotrophomonas* (Fig. S-1). Members of this genus are known to play an essential role in elements' biogeochemical cycles in nature, as is the case for sulfur (Ikemoto et al., 1980; Banerjee and Yesmin, 2002) or nitrogen (Park et al., 2005), presenting also high biotechnological potential as bioremediation agents (reviewed in Ryan et al., 2009; Ruiz-Fresneda et al., 2018, 2019). However, few *Stenotrophomonas* strains (*S. maltophilia* JG-2, *S. maltophilia* P-8-1 and P-8-3c, and *Stenotrophomonas* sp. U18) have been distinguished for their U immobilization ability (Merroun and Selenska-Pobell, 2008; Nazina et al., 2010; Islam and Sar, 2016).

The MIC of different metals for the growth of this strain was also determined for assessing tolerance of Br8 to these inorganic contaminants (Table 1). Although this method is standardly used (Wiegand et al., 2008; Sánchez-Castro et al., 2017a; Li et al., 2019), it should be noted that a minimum part of the metal assayed might be un-bioavailable due to abiotic interactions with medium components. Silver appears to be the most toxic, since no growth was detected for all tested concentrations (the minimum being 0.25 mM). Selenium, on the other hand, was found to be the least toxic. In this case, the MIC was not reached since growth was observed at the maximum concentration tested (100 mM). The formation of red color precipitates in the bacterial colonies revealed the reduction of Se(IV) and formation of elemental selenium. A phylogenetically similar bacterial strain (*S. bentonitica* BII-R7; Sánchez-Castro et al., 2017b) has recently been shown to induce the reduction of Se(IV) to Se(0), forming low-solubility trigonal Se nanostructures (Ruiz-Fresneda et al., 2018), which could explain the high tolerance of *Stenotrophomonas* strains to this element. Likewise in the case of U, MIC was not determined since the maximum concentration tested (4 mM) did not limit the cell growth. No further concentrations were tested, since heavy metals levels reported for real polluted scenarios were much lower than the concentrations assayed in the present study. The maximum tolerated U concentration for the above mentioned strain BII-R7 was 6 mM (López-Fernández et al., 2014). Such high levels of tolerance to heavy metals (e.g. U) and antibiotics in members of this genus have been underlined in other studies (reviewed in Page et al., 2008; Ryan et al., 2009; Nazina et al., 2010; Islam and Sar, 2011, 2016). It may be that a cluster of genes is involved in antibiotic and heavy metal resistance, typically from gram-positive bacteria, as found for *S. maltophilia* D457R (Alonso et al., 2000).

3.2. Bacterial immobilization of uranium

The U removal capacity of the strain Br8 was determined by means of ICP-MS. In the presence of Br8 cells and G2P (5 mM), U removal rates around 90% (maximum of 94.7%) were observed for all U concentrations tested (0.01, 0.1, 0.5 and 1 mM) at 48 h (pH 6.3, 28 °C, 165 rpm) (Fig. 1). Although no variation was detected in pH level during the incubation, abiotic controls showed U immobilization values between 10% and 30%, except at the lowest U concentration (0.01 mM), where abiotic precipitation accounted for 60% of the total U removal (Fig. 1). Heat-killed biomass controls exhibited 11% and 54% U removal in the presence of 1 mM and 0.1 mM U, respectively (Fig. 1). Although for 0.1 mM the removal rate was much higher with inactive cells than with no cells, in the case of 1 mM U no significant differences were observed for the two treatments. These results suggest that the cells of this strain interact with U through active (e.g. biomineralization) and passive (e.g. biosorption) mediated processes, as was confirmed by U kinetics studies (see results below).

The combination of different interaction mechanisms for U immobilization seems reasonable when a bacterial consortium is occurring, but numerous studies confirmed also this ability for single microbial strains (Song et al., 2019). Regarding U immobilization efficiency, a limited number of studies have reported removal rates similar to those presented here, in the presence of such high U concentrations and G2P (e.g. 95% removal for 0.5 mM initial U concentration). When considering lower initial U concentrations, bacterial strains like *Rahnella* sp. Y9602, *Leifsonia* sp. J5, or *Serratia* sp. OT−II−7, all isolated from U-rich environments, also showed U immobilization rates over 90% under different incubation conditions (Beazley et al., 2007; Chandwadkar et al., 2018; Ding et al., 2018). Moreover, three *Xanthomonadales* isolates (*Stenotrophomonas maltophilia* P-8-1 and P-8-3c, and *Rhodanobacter* sp. A2-61), likewise recovered from mining or waste disposal sites, showed much lower immobilization rates (Nazina et al., 2010; Sousa et al., 2013).

Regarding the U removal capacity of *Stenotrophomonas* sp. Br8 expressed by dry biomass weight, it was observed that 1 g of this bacterium was able to immobilize 373 mg of U after 48 h at 28 °C from a solution containing U (0.5 mM) and G2P (5 mM) at pH 6.3. Although most of previous studies report lower or similar values, e.g. *Bacillus cereus* 12−2 at pH 5 (448 mg U/g dry biomass; Zhang

Table 1
Heavy metals/metalloids minimum inhibitory concentration (MIC), in milliMolar (mM), of the bacterial isolate Br8.

Metal	Cr	Pb	La	Cd	Ni	Zn	Se	Mo	Va	Eu	Cu	Ag	U
mM	≥16	≥16	≥16	≥2	8	≥8	≥100[a]	≥8	≥8	≥4	8	<0,25	≥4

Due to possible abiotic HMMs precipitation, it was impossible to reach the final MIC value in most cases.
[a] 100 mM was used instead of 128 mM to avoid abiotic precipitation of the metal.

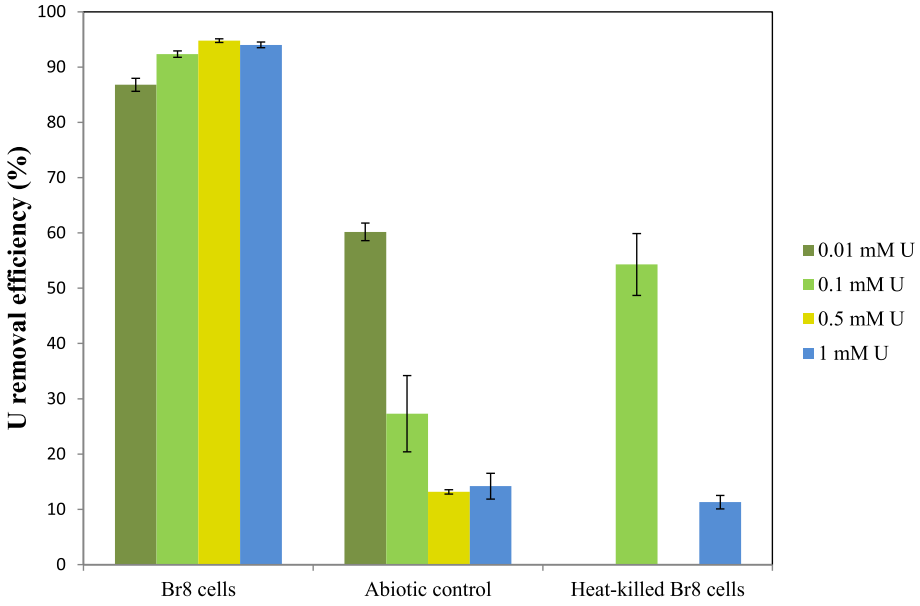

Fig. 1. Uranium removal efficiency (%) after incubation (48h; 28 °C; 165 rpm) of MOPS-buffered (20 mM) distilled water (pH 6.3) amended with G2P (5 mM) and various U concentrations (0.01, 0.1, 0.5 and 1 mM) in presence of *Stenotrophomonas* sp. Br8 cells (0.5 mg dry biomass per ml of medium, equivalent $OD_{600nm} \approx 0.5$). Flasks without cells and including heat-killed bacterial cells were used as control treatments. The data are showed as the mean ± SD of at least three independent measurements.

et al., 2018), *Paenibacillus* sp. JG-TB8 under anoxic conditions (138 mg U/g dry biomass; Reitz et al., 2014), or *B. thuringiensis* strains (400 mg U/g dry biomass; Pan et al., 2015), extreme loading capacity was observed in the engineered bacterial strain *Deinococcus radiodurans*-PhoK at 10 mM U (10700 mg U/g dry biomass; Kulkarni et al., 2013).

3.3. Phosphatase activity and inorganic phosphate release

Stenotrophomonas species are known to express P-ase activity (Sánchez-Castro et al., 2017b; Weber et al., 2018). Therefore, the role of this enzyme in the removal of U by its precipitation as U phosphates was investigated for other bacterial strains (Kulkarni et al., 2016; Chandwadkar et al., 2018; Zhang et al., 2018; Shukla et al., 2019). The P-ase activity of Br8-strain cells exposed to different U concentrations (0.01, 0.1, 0.5 and 1 mM) for 48 h, in presence of G2P, was assessed. Results showed that the enzymatic activity depends upon U concentration, being twice as high at 0.1 and 0.5 mM U concentration than at 1 mM U (Fig. 2). Although the presence of U may enhance microbial P-ase activity as a protective strategy against the U toxicity, certain concentrations of this metal seem to hinder this defense mechanism, as previously reported for uranyl ion (Macaskie et al., 2000) and other heavy metal ions such as VO_4^{3-}, Hg^{2+} and Mg^{2+} (Swarup et al., 1982; Tabaldi et al., 2007; Xu et al., 2018). In addition, low P-ase activity was exhibited by heat-killed cells, U untreated cells and low-U concentration (0.01 mM) treated cells (Fig. 2).

This Br8-inherent enzymatic activity is responsible for releasing orthophosphates, by using G2P, which may precipitate U(VI) as uranyl phosphate minerals. It should be noted that other organic phosphate sources than G2P like sodium glycerophosphate have been demonstrated to play the same role in presence of bacterial phosphatase activity (Tu et al., 2019). The amount of the orthophosphate detected after incubation increased as the U

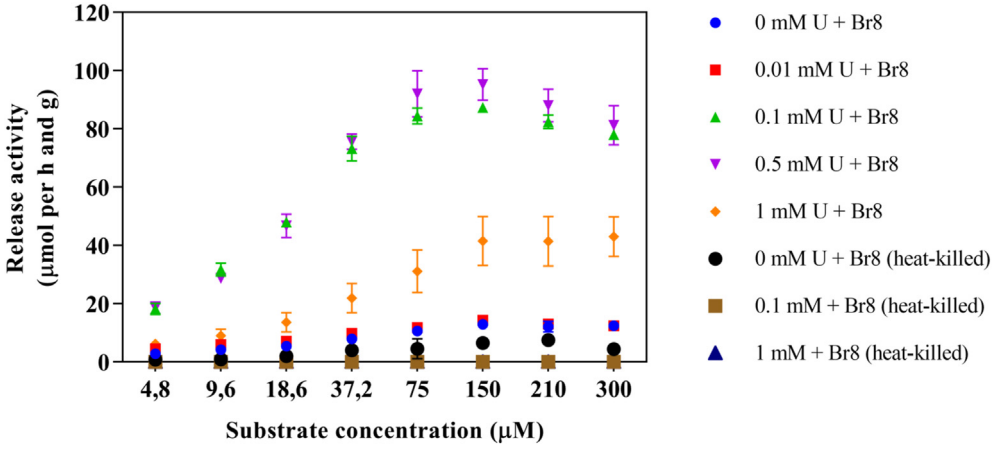

Fig. 2. Phosphatase activity (measured as µmol released per h and g at different substrate concentrations) of Br8 cells (0.5 mg dry biomass per ml of medium, equivalent $OD_{600nm} \approx 0.5$) after incubation (48h; 28 °C; 165 rpm) in MOPS-buffered (20 mM) distilled water (pH 6.3) amended with G2P (5 mM) and various U concentrations (0, 0.01, 0.1, 0.5 and 1 mM). Flasks with heat-killed bacterial cells were used as control treatment. The data are showed as the mean ± SD of at least three independent measurements.

concentration decreased (Fig. S-2). Abiotic and killed-cells controls showed very low values of released orthophosphate, a finding supported by the P-ase activity results shown above (Fig. 2).

3.4. STEM-HAADF analysis

The STEM-HAADF/EDX technique was used to determine the cellular location of U precipitated by the bacterium Br8 and to elucidate the key mechanism through which this strain copes with the radionuclide's toxicity. Micrographs of ultrathin sections of 0.1 and 1 mM U-treated-cells of *Stenotrophomonas* sp. Br8 (48 h, pH 6.3, 5 mM G2P) are presented in Fig. 3. Needle-like U precipitates were localized at the cell surface and in the extracellular space. No intracellular U accumulation was observed, suggesting the ability of this strain to overcome U toxicity by avoiding its uptake. The precipitation of U around the cell surface is probably due to the localization of P-ase enzymes at this level and, consequently, to the potential abundance of phosphate groups (Kulkarni et al., 2016; Chandwadkar et al., 2018). Potentiometric titration of the cells of a similar strain (*S. bentonitica* BII-R7) revealed a high amount of phosphate groups at the cell surface, 10.78 ± 0.31 × 10^{-4} mol/g higher than those of other bacterial strains (Ruiz-Fresneda, submitted to Environmental Science and Technology). In general, microbes inhabiting U contaminated environments accumulate biogenic metal minerals in the extracellular space as a defensive mechanism. A similar strategy was observed for *Stenotrophomonas* sp. U18 when incubated for 1h in a solution containing U (Islam and Sar, 2016). Intracellular U-containing accumulates have been observed in the closely-related bacterial strain *S. maltophilia* JG-2, isolated from U mining wastes (Merroun and Selenska-Pobell, 2008).

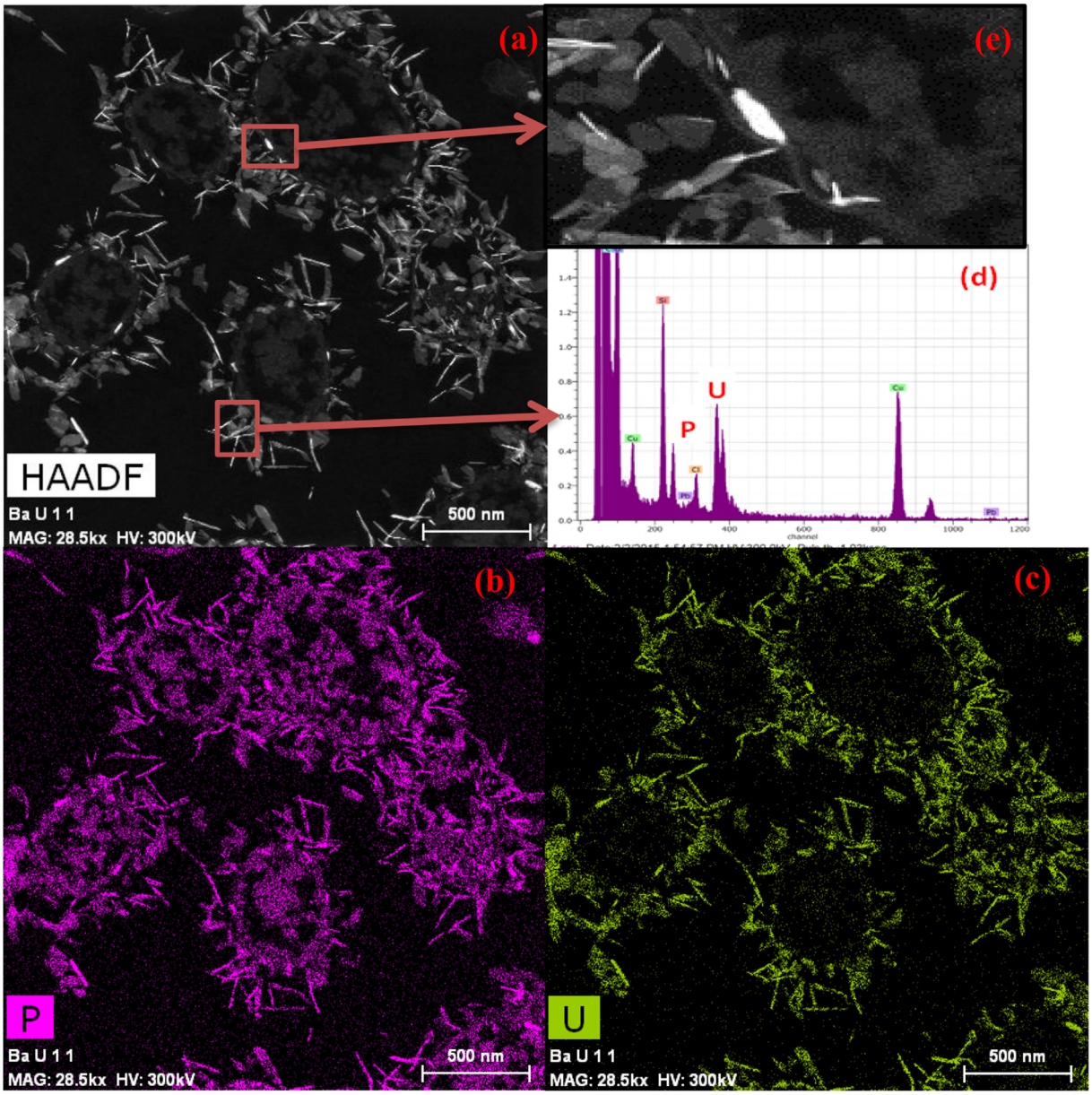

Fig. 3. HAADF-STEM micrograph (a) of a thin section showing U precipitates around Br8 cells recovered after their incubation (48h; 28 °C; 165 rpm) in MOPS-buffered (20 mM) distilled water (pH 6.3) amended with G2P (5 mM) and U (1 mM). EDX element-distribution maps for P (b) and U (c), and EDXS spectrum (d) of the point marked with a red square in (a) image, indicated that precipitates observed are mainly composed of P and U. Zoomed-in view (e) showed U precipitates located at cell surface level. . (For interpretation of the references to color in this figure legend, the reader is referred to the Web version of this article.)

EDX spectra and elemental mapping analysis indicated that the electron-dense accumulations observed extracellularly and on the cell surface are composed mainly of U and P (Fig. 3). These observations confirm the high P-ase activity of this bacterial strain and its key role in the formation of U-phosphate minerals, which are considered to be very stable for long periods over a wide range of pH, and to not re-oxidize and re-mobilize easily as is the case for U reduction byproducts (Lloyd et al., 2002; Senko et al., 2002; Beazley et al., 2011).

3.5. EXAFS analysis

The LIII-edge EXAFS spectra of the U complexes formed by Br8 cells at 0.1 and 1 mM metal concentration, and that of inorganic uranyl phosphate (m-autunite) used as a standard compound for comparison, along with their Fourier Transforms (FT), are presented in Fig. 4. The EXAFS spectra of the two experimental samples highly resemble each other and the m-autunite spectrum, indicating that the local coordination of U(VI) within the two samples consists of U phosphates.

The FT of the EXAFS spectra of the two U bacterial samples show 5 significant peaks (Fig. 4). Quantitative fit results (Table 2) (distances are phase shift corrected) showed that U(VI) has two O_{ax} at a distance of 1.78 Å and 4 O_{eq} at 2.29 ± 0.02 Å. The second peak of the FTs (R+Δ~1.8 Å) was related to the backscattering contribution of the equatorial oxygen atoms. The MS path of the axial oxygen atoms, as well as the SS and MS of the phosphate atoms, can be seen in the FTs in the region between R+Δ = 2.8 and 3.4 Å, respectively. The U-Oeq bond distance in the two samples is within the range of previously reported values for the oxygen atom of the phosphate bound to uranyl (Merroun et al., 2003, 2011; Nedelkova et al., 2007). The fourth FT peak, which appears at R+Δ ~3 Å (radial distance R = 3.61 Å) is a result of back-scattering from phosphorus atoms. This distance is typical for a monodentate coordination of U(VI) by phosphate. A fifth peak at bond distance of 5.20–5.22 ± 0.02 Å was fitted to a U–U. The EXAFS spectra of the U-treated bacterial cell samples at 2 U concentrations are similar to that of m-autunite with regard to the U-Oeq, U–P and U–U distances, suggesting that an inorganic m-autunite-like uranyl phosphate phase was precipitated by the Br8 cells in these two samples.

Table 2
Structural parameters of the uranium complexes formed by the cells of the strain *Stenotrophomonas* sp. Br8 exposed to 1 and 0,1 mM U(VI), pH 5.5 and in presence of G2P.

Sample	Shell	N[a]	R(Å)[b]	σ^2 (Å^2)[c]	ΔE (eV)
Br8/G2P/1mMU	U-O_{ax}	2[d]	1.78	0.0037	0.82
	U-O_{eq1}	3.7 ± 0,2	2.29	0.0032	
	U–P	5.5 ± 1,7	3.61	0.0093	
	U- O_{eq1}-P (MS)	11,0[e]	3.71	0.0093[f]	
	U–U	2.7 ± 1.7	5.22	0.008[d]	
Br8/G2P/0.1mMU	U-O_{ax}	2[d]	1.78	0.0043	0.42
	U-O_{eq1}	4.1 ± 0.3	2.29	0.0051	
	U–P	2.6 ± 0.7	3.61	0.0024	
	U- O_{eq1}-P (MS)	5.2[e]	3.71	0.0024[f]	
	U–U	2.1 ± 0.9	5.20	0.008[d]	

[a] Errors in coordination numbers are ±25%, and standard deviations, as estimated by EXAFSPAK, are given in parentheses.
[b] Errors in distance are ±0.02 Å.
[c] Debye-Waller factor.
[d] Value fixed for calculation.
[e] Coordination numbers for U–P and U-Oeq1-P MS were linked.
[f] Debye Waller factors for U–P and U-Oeq1-P MS were linked.

These results are in agreement with those obtained on the high P-ase activity of the Br8 strain, leading to the release of inorganic phosphate needed for U precipitation as U phosphate phases, with a local coordination similar to that of m-autunite.

3.6. Uranium-immobilization performance by Br8-cells: influencing factors

3.6.1. Time: kinetics of the uranium immobilization process

The uranium removal capacity of the strain Br8 monitored at different incubation times is presented in Fig. 5. The results indicate increased U removal rate of 16.2, 20.7 and ≈ 50% after 5, 30 and 180 min, respectively, stabilizing at ≈98% after 20 h. Abiotic controls showed a background U precipitation of ≈3–4% at 10 min, reaching values around 10%–15% after 24 h (Fig. 5). Orthophosphates in solution are first detected at a significant concentration at 24 h (Fig. S-3), once the U(VI) precipitation percentage had reached its maximum (Fig. 5).

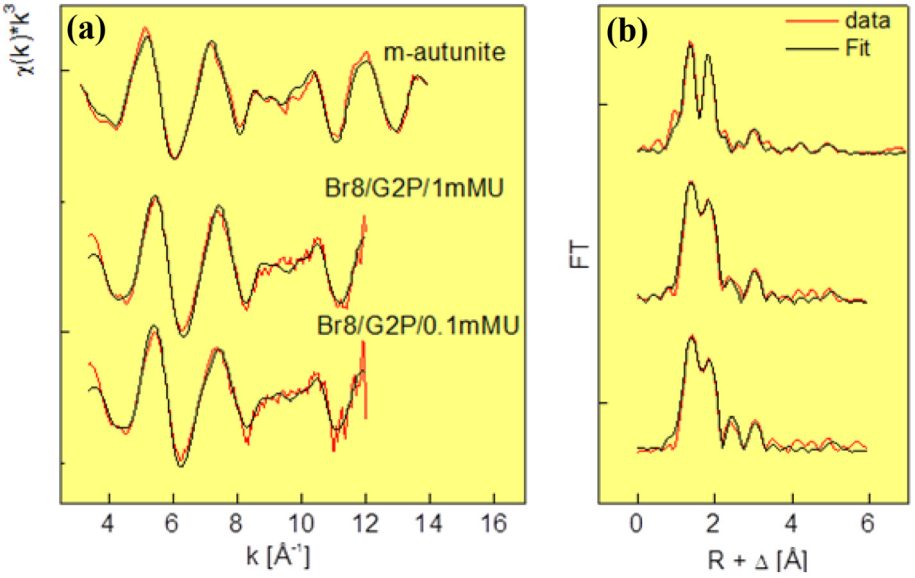

Fig. 4. (a) Uranium L_{III}-edge k^3–weighted EXAFS spectra and (b) the corresponding Fourier Transforms (FT) of the uranium complexes formed by *Stenotrophomonas* sp. Br8 cells at U concentrations of 1 mM and 0.1 mM in MOPS-buffered (20 mM) distilled water amended with G2P (5 mM), and reference compound (m-autunite).

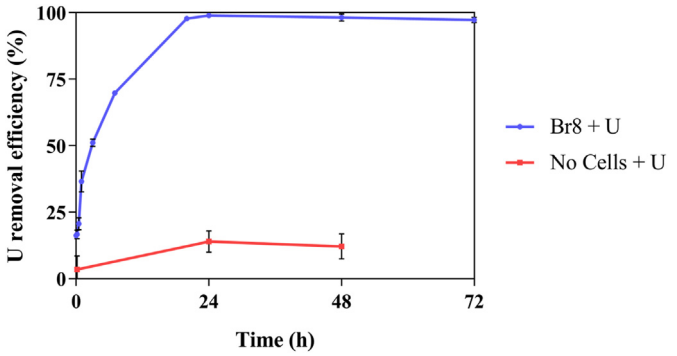

Fig. 5. Uranium removal efficiency (%) kinetics during incubation (72 h; 28 °C; 165 rpm) of MOPS-buffered (20 mM) distilled water (pH 6.3) amended with G2P (5 mM) and U (0.5 mM) in presence of *Stenotrophomonas* sp. Br8 cells (0.5 mg dry biomass per ml of medium, equivalent $OD_{600nm} \approx 0.5$). Flasks without cells were used as control treatment. The data are showed as the mean ± SD of at least three independent measurements.

As suggested above, these findings support the implication of active and passive mechanisms in aerobic U immobilization. Metabolically independent mechanisms likely based on U sorption onto the cell surface of the bacterium are first to be detected in this time-course experiment. Previous reports describe similarly fast actinides sequestration, interpreting them as passive events (Gerber et al., 2016; Shukla et al., 2017). A large number of bacterial functional groups at the cell surface (e.g. carboxyl, hydroxyl, amino and phosphoryl) are known to effectively provide binding sites for metals and other toxic elements (Fein et al., 2005; Ojeda et al., 2008; Merroun et al., 2011; Moll et al., 2014; Reitz et al., 2015). Phosphate groups have been found to be particularly abundant at the cell surface level in the Br8 closely related bacterial strain *S. bentonitica* BII-R7 in comparison to other bacteria (Ruiz-Fresneda, submitted to Environmental Science and Technology). In terms of biomineralization active mechanisms, the lack of orthophosphates in excess in the incubation medium before 24 h suggests that the process kinetics at this U concentration are governed by the rate of release of enzymatic inorganic phosphates. While soluble U(VI) is available in the system, free orthophosphates bound rapidly to it, making its detection impossible. Subsequent sampling times (48 and 72 h) show a linear increase of orthophosphates in the medium (Fig. S-3), indicating a continuous orthophosphates release via P-ase activity. No-cell control treatments evidenced an abiotic removal process most likely produced by spontaneous chemical conversion of G2P into orthophosphates, which may interact with the solved U fraction. This background abiotic U removal (approx. 10%–15%) was repeatedly obtained in our work.

3.6.2. Biomass concentration

The effect of biomass concentration (0.25, 0.5 and 1 mg/mL dry biomass) in the U immobilization process was investigated to determine the optimal Br8 cell concentration for removing U in solution in the presence of G2P. The uranium precipitation ability of this strain was not affected by this biological parameter. Removal rates at the studied biomass concentrations (0.25, 0.5 and 1 mg/mL dry weight) did not differ significantly (Fig. S-4a). Even at the lowest concentration (0.25 mg/mL dry weight), U removal (94.8%) remained at the same level as in previous assays (Fig. S-4a). However, the measured concentrations of orthophosphates released in the medium varied clearly depending on the biomass concentration (Fig. S-4b). These changes in the amount of inorganic phosphates released are not proportional to the biomass concentration, indicating a nonlinear relationship. Considering these results, limitation of the U biomineralization process is imposed by Br8 enzymatic activity and not by the G2P concentration, which is clearly in excess in our experiments. Since the minimum biomass concentration tested in this case (0.25 mg/mL dry weight) resulted in maximum U removal values, further optimization experiments are needed to determine the minimum biomass applicable for satisfactory U removal rates.

3.6.3. pH

The effect of pH in the U biomineralization mediated by Br8 cells was also investigated in order to determine whether this process is suitable for bioremediation of acidic or alkaline U contaminated waters. For this purpose, slightly acidic (pH 5) and alkaline (pH 8) conditions were investigated. Similar U removal rates (93%–99%; Fig. S-5a) as those observed in previous experiments at circumneutral pH (92%–95%; Fig. 1) were obtained for acidic and alkaline pH conditions, regardless of the U concentrations assayed (0.1, 0.5 and 1 mM U) (Fig. S-5a). The chemical speciation of U in the studied systems (Tables S–1) showed that at pH 5, U largely formed positively charged uranium hydroxide complexes (e.g. $(UO_2)_3(OH)^{5+}$, UO_2^{2+}, UO_2OH^+, $(UO_2)_2(OH)_2^{2+}$), while at pH 8, the negatively charged uranyl hydroxide $(UO_2)_3(OH)^{7-}$ occurred also in a significant proportion (14.6–18.5%, depending on U initial concentration; Tables S–1). Thus, the passive initial phase of U biosorption is expectable to be more pronounced under slightly acidic pH, where the positively charged hydroxide complexes are more represented, rather than under pH 8. Concerning active mechanisms, the release of orthophosphates by Br8 cells was higher at alkaline pH, where an excess of orthophosphates in solution was detected for all U concentrations at 48 h (Fig. S-5b). Under acidic conditions, the inorganic phosphate concentration in solution decreased significantly at all U concentrations. Yet it should be noted that even under these conditions, the cells released sufficient orthophosphates to precipitate most of the U in solution (94.6% for 1 mM initial U concentration). The measurements of P-ase activity gave values of 40 μmol (per h and g) at both alkaline and acidic pHs for all three U concentrations tested, except in the case of pH 5 and 0.5 mM U, where this activity showed a maximum value of 60–62 μmol (per h and g).

Since previous experiments at circumneutral pH showed higher P-ase activity (Fig. 2), in accordance with previous investigations (Macaskie et al., 1994; Kulkarni et al., 2016), we hypothesize that at these pH conditions both types of phosphatases may act with a summative effect. The unexpected high P-ase activity associated with low levels of orthophosphates released seen at pH 5 and 0.5 mM U would indicate a reduction in the efficiency of Br8 enzymatic activity. Similar contradictory results were recently reported by Chandwadkar et al. (2018), who observed slower U precipitation kinetics at pH 5 but a higher P-ase activity when compared to the same test at pH 7 and 9. Several studies with enterobacteria demonstrate that a high P-ase activity is not enough to confer metal immobilization properties (Macaskie et al., 1994; Jeong and Macaskie, 1995). *Serratia* bacterial cells were found to be damaged and lysed at pH 5, allowing solved uranyl to penetrate and precipitate within the cytoplasm (Chandwadkar et al., 2018), likely affecting the sensitive P-ase activity (Macaskie et al., 2000). On the other hand, at alkaline pH (8), the presence of carbonates may hinder uranyl phosphate precipitation because of the formation of highly soluble uranyl carbonate complexes (Nilgiriwala et al., 2008; Kulkarni et al., 2016). At any rate, no intracellular U precipitates are normally found under these alkaline conditions, maintaining cell viability intact (Kulkarni et al., 2016).

Since U removal values at pH 8 resulted slightly higher than those obtained under circumneutral and acidic conditions (Figs. S-5a and 1), microscopic STEM observations were made to investigate

the interaction mechanisms involved in this case. Microscopy images (Fig. S-6) reveal the presence of flake-shaped accumulates, located extracellularly and at the cell surface level, larger than those found previously under circumneutral conditions (Fig. 3). Similarly to those analyzed before at pH 6.3, EDX spectra and elemental mapping analysis indicated that the precipitates formed are composed mainly of U and P (Fig. S-6). Through XRD analysis, structures resembling $Rb[(UO_2)(PO_4)](H_2O)_3$ and autunite $[CaU(PO_4)_2]$ were identified in the precipitates resulting under alkaline and acidic conditions, respectively (Fig. S-7).

3.6.4. Temperature

Regarding the temperature effect in the bio-immobilization process at 48 h, maximum removal efficiencies (>90%) were observed at 28 °C and 37 °C (Fig. S-8a). Orthophosphate concentrations measured at 48 h (Fig. S-8b) suggest higher enzymatic activity at 37 °C. At 15 °C, Br8 U precipitation ability decreased approximately 20% (Fig. S-8a).

For most mesophiles, metabolic capacity in general and P-ase enzymatic activity in particular are known to be reduced when temperature drops under 20 º-25 °C (González et al., 1994; Lee et al., 2015; Behera et al., 2017). As pointed out in the previous section, the U removal mechanism reported in this work is highly dependent upon the metabolic capacity of Br8 cells, which is clearly higher at moderate temperatures (28 º- 37 °C) than at lower ones such as 15 °C.

4. Conclusions

This study describes a highly efficient process for soluble U(VI) immobilization mediated by a bacterial strain from the genus *Stenotrophomonas* (Br8) in presence of G2P as organophosphate source at different pH values (5, 7 and 8). Although U removal from aqueous solutions mediated by certain bacterial strains in presence of an organophosphate compound has already been reported (Macaskie et al., 1992, 1994; Beazley et al., 2007, 2009; Martinez et al., 2007; Merroun et al., 2011), the present work demonstrates the ability of the strain Br8 for tolerating and immobilizing aerobically high U concentrations in a short period of time under changing environmental conditions. The biogenic U phosphate phases precipitated by this strain presented a local coordination similar to that of autunite groups, characterized by their high long-term stability.

In summary, these results have direct implications for understanding bacterial U tolerance mechanisms and the impact of the strain *Stenotrophomonas* sp. (Br8) on mobility and biogeochemical U cycling in nature. They also demonstrate the potential of this bacterial strain for U bioremediation as a result of a complex process combining passive and active mechanisms, including fast biosorption to the cell surfaces and a subsequent P-ase enzyme-mediated biomineralization phase (e.g. Chandwadkar et al., 2018). Moreover, since phosphatases are also activated under anaerobic conditions (Rossolini et al., 1998), the U biomineralization presented here may be an alternative to bioreduction in the presence of G2P when the presence of oxygen is limited. Despite these promising data presented, further research is needed on the performance of this process when applied to real U-polluted mining waters through column experiments for the design of appropriate application procedures.

CRediT AUTHOR STATEMENT

Iván Sánchez-Castro: Methodology, Investigation, Writing - original draft, Validation, Formal analysis, Visualization, Software, Writing - review & editing. **Pablo Martínez-Rodríguez**: Methodology, Investigation, Formal analysis, Visualization, Software, Writing - review & editing. **Fadwa Jroundi**: Writing - review & editing. **Pier Lorenzo Solari**: Methodology, Investigation, Formal analysis, Visualization, Software, Writing - review & editing. **Michael Descostes**: Conceptualization, Validation, Formal analysis, Visualization, Software, Resources, Writing - review & editing. **Mohamed L. Merroun**: Conceptualization, Methodology, Investigation, Validation, Formal analysis, Visualization, Software, Resources, Writing - review & editing, Supervision.

Declaration of competing interest

The authors declare that they have no known competing financial interests or personal relationships that could have appeared to influence the work reported in this paper.

Acknowledgements

This work was supported by ORANO Mining (France) [collaborative research contract nº 3022 OTRI-UGR]. It results from a Joint Research Project between Orano Mining R&D Department and the Department of Microbiology of the University of Granada. We acknowledge the assistance at the STEM-HAADF and XRD measurements of Maria del Mar Abad Ortega, Concepción Hernández Castillo and José Romero Garzón (Centro de Instrumentación Científica, University of Granada, Spain). We also acknowledge SOLEIL for provision of synchrotron radiation facilities.

Appendix A. Supplementary data

Supplementary data to this article can be found online at https://doi.org/10.1016/j.watres.2020.116110.

References

Acharya, C., 2015. Uranium bioremediation: approaches and challenges. In: Sukla, L.B., Pradhan, N., Panda, S., Mishra, B.K. (Eds.), Environmental Microbial Biotechnology, pp. 119–132. http://www.springer.com/978-3-319-19017-4.

Alonso, A., Sanchez, P., Martinez, J.L., 2000. *Stenotrophomonas maltophilia* D457R contains a cluster of genes from Gram-positive bacteria involved in antibiotic and heavy metal resistance. Antimicrob. Agents Chemother. 44, 1778–1782.

Ankudinov, A., Ravel, B., Rehr, J., Conradson, S., 1998. Real-space multiple-scattering calculation and interpretation of x-ray-absorption near-edge structure. Phys. Rev. B 58, 7565.

Bader, M., Müller, K., Foerstendorf, H., Drobot, B., Schmidt, M., Musat, N., Swanson, J., Reed, D., Stump, T., Cherkouk, A., 2017. Multistage bioassociation of uranium onto an extremely halophilic archaeon revealed by a unique combination of spectroscopic and microscopic techniques. J. Hazard Mater. 327, 225–232.

Banerjee, M., Yesmin, L., 2002. Sulfur-oxidizing plant growth promoting rhizobacteria for enhanced canola performance. US Patent, 07491535.

Bargar, J.R., Bernier-Latmani, R., Giammar, D.E., Tebo, B.M., 2008. Biogenic uraninite nanoparticles and their importance for uranium remediation. Elements 4, 407–412.

Beazley, M.J., Martinez, R.J., Sobecky, P.A., Webb, S.M., Taillefert, M., 2007. Uranium biomineralization as a result of bacterial phosphatase activity: insights from bacterial isolates from a contaminated subsurface. Environ. Sci. Technol. 41, 5701–5707.

Beazley, M.J., Martinez, R.J., Sobecky, P.A., Webb, S.M., Taillefert, M., 2009. Non-reductive biomineralization of uranium(VI) phosphate via microbial phosphatase activity in anaerobic conditions. Geomicrobiol. J. 26, 431–441. https://doi.org/10.1080/01490450903060780.

Beazley, M.J., Martinez, R.J., Webb, S.M., Sobecky, P.A., Taillefert, M., 2011. The effect of pH and natural microbial phosphatase activity on the speciation of uranium in subsurface soils. Geochem. Cosmochim. Acta 75, 5648–5663.

Behera, B.C., Yadav, H., Singh, S.K., Mishra, R.R., Sethi, B.K., Dutta, S.K., Thatoi, H.N., 2017. Phosphate solubilization and acid phosphatase activity of *Serratia* sp. isolated from mangrove soil of Mahanadi river delta, Odisha, India. J. Genet. Eng. Biotechnol. 15, 169–178.

Chandwadkar, P., Misra, H.S., Acharya, C., 2018. Uranium biomineralization induced by a metal tolerant *Serratia* strain under acid, alkaline and irradiated conditions. Metall 10, 1078–1088.

Ding, L., Tan, W.-F., Xie, S.-B., Mumford, K., Lv, J.-W., Wang, H.-Q., Fang, Q., Zhang, X.-W., Wu, X.-Y., Li, M., 2018. Uranium adsorption and subsequent re-oxidation under aerobic conditions by Leifsonia sp. - coated biochar as green trapping

agent. Environ. Pollut. 242, 778–787.
Fein, J.B., Boily, J.-F., Yee, N., Gorman-Lewis, D., Turner, B.F., 2005. Potentiometric titrations of *Bacillus subtilis* cells to low pH and a comparison of modeling approaches. Geochem. Cosmochim. Acta 69, 1123–1132.
Gavrilescu, M., Pavel, L.V., Cretescu, I., 2009. Characterization and remediation of soils contaminated with uranium. J. Hazard Mater. 163, 475–510.
Gerber, U., Zirnstein, I., Krawczyk-Bärsch, E., Lünsdorf, H., Arnold, T., Merroun, M.L., 2016. Combined use of flow cytometry and microscopy to study the interactions between the gram-negative betaproteobacterium *Acidovorax facilis* and uranium (VI). J. Hazard Mater. 317, 127–134.
German, D.P., Weintraub, M.N., Grandy, A.S., Lauber, C.L., Rinkes, Z.L., Allison, S.D., 2011. Optimization of hydrolytic and oxidative enzyme methods for ecosystem studies. Soil Biol. Biochem. 43, 1387–1397.
González, D.F., Fárez-Vidal, M.E., Arias, J.M., Montoya, E., 1994. Partial purification and biochemical properties of acid and alkaline phosphatases from *Myxococcus coralloides*. J. Appl. Bacteriol. 77, 567–573.
Hsi, C.D., Langmuir, D., 1985. Adsorption of uranyl onto ferric oxyhydroxides: application of the surface complexation site-binding model. Geochem. Cosmochim. Acta 49, 1931–1941. https://doi.org/10.1016/0016-7037(85)90088-2.
Hudson, E., Allen, P., Terminello, L., Denecke, M., Reich, T., 1996. Polarized x-ray-absorption spectroscopy of the uranyl ion: comparison of experiment and theory. Phys. Rev. B 54, 156.
Ikemoto, S., Suzuki, K., Kaneko, T., Komagata, K., 1980. Characterization of strains of *Pseudomonas maltophilia* which do not require methionine. Int. J. Syst. Bacteriol. 30, 437–447.
Islam, E., Sar, P., 2011. Culture-dependent and -independent molecular analysis of bacterial community within uranium ore. J. Basic Microbiol. 51, 1–13.
Islam, E., Sar, P., 2016. Diversity, metal resistance and uranium sequestration abilities of bacteria from uranium ore deposit in deep earth stratum. Ecotoxicol. Environ. Saf. 127, 12–21.
Jeong, B.C., Macaskie, L.E., 1995. PhoN-type acid phosphatases of a heavy metal-accumulating *Citrobacter* sp.: resistance to heavy metals and affinity towards phosphomonoester substrates. FEMS Microbiol. Lett. 130, 211–214.
Kolhe, N., Zinjarde, S., Acharya, C., 2018. Responses exhibited by various microbial groups relevant to uranium exposure. Biotechnol. Adv. 36, 1828–1846.
Kong, L., Ruan, Y., Zheng, Q., Su, M., Diao, Z., Chen, D., Hou, L.A., Chang, X., Shih, K., 2020. Uranium extraction using hydroxyapatite recovered from phosphorus containing wastewater. J. Hazard Mater. 382, 120784.
Krawczyk-Bärsch, E., Gerber, U., Müller, K., Moll, H., Rossberg, A., Steudtner, R., Merroun, M.L., 2018. Multidisciplinary characterization of U(VI) sequestration by *Acidovorax facilis* for bioremediation purposes. J. Hazard Mater. 347, 233–241.
Kulkarni, S., Ballal, A., Apte, S.K., 2013. Bioprecipitation of uranium from alkaline waste solutions using recombinant *Deinococcus radiodurans*. J. Hazard Mater. 262, 853–861.
Kulkarni, S., Misra, C.S., Gupta, A., Ballal, A., Apte, S.K., 2016. Interaction of uranium with bacterial cell surfaces: inferences from phosphatase-mediated uranium precipitation. Appl. Environ. Microbiol. 82, 4965–4974.
Langmuir, D., 1978. Uranium solution-mineral equilibria at low temperatures with applications to sedimentary ore deposits. Geochem. Cosmochim. Acta 42, 547–569.
Lee, D.-H., Choi, S.-L., Rha, E., Kim, S.J., Yeom, S.-J., Moon, J.-H., Lee, S.-G., 2015. A novel psychrophilic alkaline phosphatase from the metagenome of tidal flat sediments. BMC Biotechnol. 15, 1.
Li, X., Gu, A.Z., Zhang, Y., Xie, B., Li, D., Chen, J., 2019. Sub-lethal concentrations of heavy metals induce antibiotic resistance via mutagenesis. J. Hazard Mater. 369, 9–16.
Lloyd, J.R., Chesnes, J., Glasauer, S., Bunker, D.J., Livens, F.R., Lovley, D.R., 2002. Reduction of actinides and fission products by Fe(III)-reducing bacteria. Geomicrobiol. J. 19, 103–120.
López-Fernández, M., Fernández-Sanfrancisco, O., Moreno-García, A., Martín-Sánchez, I., Sánchez-Castro, I., Merroun, M.L., 2014. Microbial communities in bentonite formations and their interactions with uranium. Appl. Geochem. 49, 77–86.
Lovley, D.R., Phillips, E.J.P., Gorby, Y.A., Landa, E.R., 1991. Microbial reduction of uranium. Nature 350, 413–416.
Lovley, D.R., Phillips, E.J.P., 1992. Bioremediation of uranium contamination with enzymatic uranium reduction. Environ. Sci. Technol. 26, 2228–2234. https://doi.org/10.1021/es00035a023.
Lovley, D.R., 2001. Bioremediation anaerobes to the rescue. Science 293, 1444–1446.
Macaskie, L.E., Empson, R.M., Cheetham, A.K., Grey, C.P., Skarnulis, A.J., 1992. Uranium bioaccumulation by a *Citrobacter* sp. as a result of enzymically mediated growth of polycrystalline e HUO_2PO_4. Science 257, 782–784. https://doi.org/10.1126/science.1496397.
Macaskie, L.E., Bonthrone, K.M., Rouch, D.M., 1994. Phosphatase-mediated heavy metal accumulation by a *Citrobacter* sp. and related enterobacteria. FEMS Microbiol. Lett. 121, 141–146.
Macaskie, L.E., Bonthrone, K.M., Yong, P., Goddard, D.T., 2000. Enzymically mediated bioprecipitation of uranium by a *Citrobacter* sp.: a concerted role for exocellular lipopolysaccharide and associated phosphatase in biomineral formation. Microbiology 146, 1855–1867.
Makarov, E., Ivanov, V., 1960. The crystalline structure of $Ca(UO_2)_2$ $(PO_4)_2.6H_2O$ meta-otenite. Dokl. Akad. Nauk SSSR 132, 673–676.
Martinez, R.J., Beazley, M.J., Taillefert, M., Arakaki, A.K., Skolnick, J., Sobecky, P.A., 2007. Aerobic uranium (VI) bioprecipitation by metal-resistant bacteria isolated from radionuclide- and metal-contaminated subsurface soils. Environ. Microbiol. 9, 3122–3133. https://doi.org/10.1111/j.1462-2920.2007.01422.x.
Mehta, V.S., Maillot, F., Wang, Z., Catalano, J.G., Giammar, D.E., 2013. Effect of co-solutes on the products and solubility of uranium(VI) precipitated with phosphate. Chem. Geol. 364, 66–75.
Merroun, M.L., Hennig, C., Rossberg, A., Reich, T., Selenska-Pobell, S., 2003. Characterization of U (VI)-*Acidithiobacillus ferrooxidans* complexes using EXAFS, transmission electron microscopy, and energy-dispersive X-ray analysis. Radiochim. Acta 91, 583–592.
Merroun, M.L., Raff, J., Rossberg, A., Hennig, C., Reich, T., Selenska-Pobell, S., 2005. Complexation of uranium by cells and S-layer sheets of *Bacillus sphaericus* JG-A12. Appl. Environ. Microbiol. 71, 5532–5543.
Merroun, M.L., Selenska-Pobell, S., 2008. Bacterial interactions with uranium: an environmental perspective. J. Contam. Hydrol. 102, 285–295.
Merroun, M.L., Nedelkova, M., Ojeda, J.J., Reitz, T., López-Fernández, M., Arias, J.M., Romero-González, M., Selenska-Pobell, S., 2011. Bio-precipitation of uranium by two bacterial isolates recovered from extreme environments as estimated by potentiometric titration, TEM and X-ray absorption spectroscopic analyses. J. Hazard Mater. 197, 1–10.
Moll, H., Lütke, L., Bachvarova, V., Cherkouk, A., Selenska-Pobell, S., Bernhard, G., 2014. Interactions of the mont terri opalinus clay isolate *sporomusa* sp. MT-2.99 with curium(III) and europium(III). Geomicrobiol. J. 31, 682–696. https://doi.org/10.1080/01490451.2014.889975.
Murphy, J., Riley, J.P., 1962. A modified single-solution method for the determination of phosphorus in natural waters. Anal. Chim. Acta 27, 31–36.
Nazina, T.N., Lukyanova, E.A., Zakharova, E.V., Konstantinova, L.I., Kalmykov, S.N., Poltaraus, A.B., Zubkove, A.A., 2010. Microorganisms in a disposal site for liquid radioactive wastes and their influence on radionuclides. Geomicrobiol. J. 27, 473–486.
Nedelkova, M., Merroun, M.L., Rossberg, A., Hennig, C., Selenska-Pobell, S., 2007. *Microbacterium* isolates from the vicinity of a radioactive waste depository and their interactions with uranium. FEMS Microbiol. Ecol. 59, 694–705.
Neill, T.S., Morris, K., Pearce, C.I., Sherriff, N.K., Burke, M.G., Chater, P.A., Janssen, A., Natrajan, L., Shaw, S., 2018. Stability, composition, and core–shell particle structure of uranium(IV)-silicate colloids. Environ. Sci. Technol. 52, 9118–9127.
Newsome, L., Morris, K., Trivedi, D., Bewsher, A., Lloyd, J.R., 2015. Biostimulation by glycerol phosphate to precipitate recalcitrant uranium(IV) phosphate. Environ. Sci. Technol. 49, 11070–11078.
Nilgiriwala, K.S., Alahari, A., Rao, A.S., Apte, S.K., 2008. Cloning and overexpression of alkaline phosphatase PhoK from *Sphingomonas* sp strain BSAR-1 for bioprecipitation of uranium from alkaline solutions. Appl. Environ. Microbiol. 74, 5516–5523.
Ojeda, J.J., Romero-González, M.E., Bachmann, R.T., Edyvean, R.G., Banwart, S.A., 2008. Characterization of the cell surface and cell wall chemistry of drinking water bacteria by combining XPS, FTIR spectroscopy, modeling, and potentiometric titrations. Langmuir 24, 4032–4040.
Page, D., Rose, J., Conrod, S., Cuine, S., Carrier, P., Heulin, T., Achouak, W., 2008. Heavy metal tolerance in *Stenotrophomonas maltophilia*. PloS One 3, e1539.
Pan, X., Chen, Z., Chen, F., Cheng, Y., Lin, Z., Guan, X., 2015. The mechanism of uranium transformation from U (VI) into nano-uramphite by two indigenous *Bacillus thuringiensis* strains. J. Hazard Mater. 297, 313–319. https://doi.org/10.1016/j.jhazmat.2015.05.019.
Park, M., Kim, C., Yang, J., Lee, H., Shin, W., Kim, S., Sa, T., 2005. Isolation and characterization of diazotrophic growth promoting bacteria from rhizosphere of agricultural crops of Korea. Microbiol. Res. 160, 127–133.
Ravel, B., Newville, M.A., 2005. ARTEMIS, hephaestus: data analysis for X-ray absorption spectroscopy using IFEFFIT. J. Synchrotron Radiat. 12, 537–541.
Reitz, T., Rossberg, A., Barkleit, A., Selenska-Pobell, S., Merroun, M.L., 2014. Decrease of U (VI) immobilization capability of the facultative anaerobic strain *Paenibacillus* sp. JG-TB8 under anoxic conditions due to strongly reduced phosphatase activity. PloS One 9, e102447.
Reitz, T., Rossberg, A., Barkleit, A., Steudtner, R., Selenska-Pobell, S., Merroun, M.L., 2015. Spectroscopic study on uranyl carboxylate complexes formed at the surface layer of *Sulfolobus acidocaldarius*. Dalton Trans. 44, 2684–2692.
Rossolini, G.M., Shipa, S., Riccio, M.L., Berlutti, F., Macaskie, L.E., Thaller, M.C., 1998. Bacterial non-specific acid phosphatases: physiology, evolution, and use as tools in microbial biotechnology. Cell. Mol. Life Sci. 54, 833–850.
Ruiz Fresneda, M.A., Delgado-Martín, J., Gómez-Bolívar, J., Fernández-Cantos, M.V., Bosch-Estévez, G., Martínez Moreno, M.F., Merroun, M.L., 2018. Green synthesis and biotransformation of amorphous Se nanospheres to trigonal 1D Se nanostructures: impact on Se mobility within the concept of radioactive waste disposal. Environ. Sci. Nano 5, 2103–2116. https://doi.org/10.1039/C8EN00221E.
Ruiz Fresneda, M.A., Gómez-Bolívar, J., Delgado-Martín, J., Abad-Ortega, M.M., Guerra-Tschuschke, I., Merroun, M.L., 2019. The bioreduction of selenite under anaerobic and alkaline conditions analogous to those expected for a deep geological repository system. Molecules 24, 3868.
Ryan, R.P., Monchy, S., Cardinale, M., Taghavi, S., Crossman, L., Avison, M.B., Berg, G., van der Lelie, D., Dow, J.M., 2009. The versatility and adaptation of bacteria from the genus *Stenotrophomonas*. Nat. Rev. Microbiol. 7, 514–525.
Sánchez-Castro, I., Amador-García, A., Moreno-Romero, C., López-Fernández, M., Phrommavanh, V., Nos, J., Descostes, M., Merroun, M.L., 2017a. Screening of bacterial strains isolated from uranium mill tailings porewaters for bioremediation purposes. J. Environ. Radioact. 166, 130–141.
Sánchez-Castro, I., Ruiz-Fresneda, M.A., Bakkali, M., Kämpfer, P., Glaeser, S.P., Busse, H.J., López-Fernández, M., Martínez-Rodríguez, P., Merroun, M.L., 2017b.

Stenotrophomonas bentonitica sp. nov., isolated from bentonite formations. Int. J. Syst. Evol. Microbiol. 67, 2779–2786. https://doi.org/10.1099/ijsem.0.002016.
Schindler, M., Lussier, A.J., Bellrose, J., Rouvimov, S., Burns, P.C., Kurt Kyser, T., 2017. Mobilization and agglomeration of uraninite nanoparticles: a nano-mineralogical study of samples from the Matoush Uranium ore deposit. Am. Mineral. 102, 1776–1787.
Senko, J.M., Istok, J.D., Suflita, J.M., Krumholz, L.R., 2002. In situ evidence for uranium immobilization and remobilization. Environ. Sci. Technol. 36, 1491–1496.
Shen, Y., Zheng, X., Wang, X., Wang, T., 2018. The biomineralization process of uranium(VI) by *Saccharomyces cerevisiae*-transformation from amorphous U(VI) to crystalline chernikovite. Appl. Microbiol. Biotechnol. 102, 4217–4229.
Shukla, A., Parmar, P., Saraf, M., 2017. Radiation, radionuclides and bacteria: an in-perspective review. J. Environ. Radioact. 180, 27–35.
Shukla, S.K., Hariharan, S., Rao, T.S., 2019. Uranium bioremediation by acid phosphatase activity of Staphylococcus aureus biofilms: can a foe turn a friend? J. Hazard Mater. 121316 https://doi.org/10.1016/j.jhazmat.2019.121316 (in press).
Sitaud, B., Solari, P.L., Schlutig, S., Llorens, I., Hermange, H., 2012. Characterization of radioactive materials using the MARS beamline at the synchrotron SOLEIL. J. Nucl. Mater. 425, 238–243.
Song, J., Han, B., Song, H., Yang, J., Zhang, L., Ning, P., Lin, Z., 2019. Nonreductive biomineralization of uranium by *Bacillus subtilis* ATCC-6633 under aerobic conditions. J. Environ. Radioact. 208–209, 106027.
Sousa, T., Chung, A.P., Pereira, A., Piedade, A.P., Morais, P.V., 2013. Aerobic uranium immobilization by *Rhodanobacter* A2-61 through formation of intracellular uranium-phosphate complexes. Metall 5, 390–397. https://doi.org/10.1039/c3mt00052d.
Spycher, N.F., Issarangkun, M., Stewart, B.D., Sevinç Şengör, S., Belding, E., Ginn, T.R., Peyton, B.M., Sani, R.K., 2011. Biogenic uraninite precipitation and its reoxidation by iron(III) (hydr)oxides: a reaction modeling approach. Geochem. Cosmochim. Acta 75, 4426–4440.
Suzuki, Y., Banfield, J.F., 1999. Geomicrobiology of uranium. In: Burns, P.C., Finch, R. (Eds.), Uranium: Mineralogy, Geochemistry and the Environment. Mineralogical Society of America, Washington, DC, pp. 393–432.
Swarup, G., Cohen, S., Garbers, D.L., 1982. Inhibition of membrane phosphotyrosyl-protein phosphatase activity by vanadate. Biochem. Bioph. Res. Co. 107, 1104–1109.
Tabaldi, L., Ruppenthal, R., Cargnelutti, D., Morsch, V., Pereira, L., Schetinger, M., 2007. Effects of metal elements on acid phosphatase activity in cucumber (*Cucumis sativus* L.) seedlings. Environ. Exp. Bot. 59, 43–48.
Tu, H., Guo, Y.Y., Zhao, C.S., Liu, J., Li, F.Z., Yang, J.J., Liao, J.L., Yang, Y.Y., Liu, N., 2019. U-phosphate biomineralization induced by *Bacillus* sp. dw-2 in the presence of organic acids. Nucl. Eng. Technol. 51, 1322–1332.
VanEngelen, M.R., Field, E.K., Gerlach, R., Lee, B.D., Apel, W.A., Peyton, B.M., 2010. UO_2^{2+} speciation determines uranium toxicity and bioaccumulation in an environmental *Pseudomonas* sp. isolate. Environ. Toxicol. Chem. 29, 763–769.
Waite, T.D., Davis, J.A., Payne, T.E., Waychunas, G.A., Xu, N., 1994. Uranium(VI) adsorption to ferrihydrite: application of a surface complexation model. Geochem. Cosmochim. Acta 58, 5465–5478. https://doi.org/10.1016/0016-7037(94)90243-7.
Wall, J.D., Krumholz, L., 2006. Uranium reduction. Annu. Rev. Microbiol. 60, 149–166.
Wan, J., Tokunaga, T.K., Brodie, E., Wang, Z., Zheng, Z., Herman, D., Hazen, T.C., Firestone, M.K., Sutton, S.R., 2005. Reoxidation of bioreduced uranium under reducing conditions. Environ. Sci. Technol. 39, 6162–6169.
Wan, J., Tokunaga, T.K., Kim, Y., Brodie, E., Daly, R., Hazen, T.C., Firestone, M.K., 2008. Effects of organic carbon supply rates on uranium mobility in a previously bioreduced contaminated sediment. Environ. Sci. Technol. 42, 7573–7579.
Wang, Z.M., Lee, S.-W.W., Kapoor, P., Tebo, B.M., Giammar, D.E., 2013. Uraninite oxidation and dissolution induced by manganese oxide: a redox reaction between two insoluble minerals. Geochem. Cosmochim. Acta 100, 24–40.
Watson, D.B., Wu, W.M., Mehlhorn, T., Tang, G.P., Earles, J., Lowe, K., Gihring, T.M., Zhang, G.X., Phillips, J., Boyanov, M.I., Spalding, B.P., Schadt, C., Kemner, K.M., Criddle, C.S., Jardine, P.M., Brooks, S.C., 2013. In situ bioremediation of uranium with emulsified vegetable oil as the electron donor. Environ. Sci. Technol. 47, 6440–6448.
Weber, M., Schünemann, W., Fuß, J., Kämpfer, P., Lipski, A., 2018. *Stenotrophomonas lactitubi* sp. nov. and *Stenotrophomonas indicatrix* sp. nov., isolated from surfaces with food contact. Int. J. Syst. Evol. Microbiol. 68, 1830–1838.
Wiegand, I., Hilpert, K., Hancock, R., 2008. Agar and broth dilution methods to determine the minimal inhibitory concentration (MIC) of antimicrobial substances. Nat. Protoc. 3, 163–175.
Wu, W.-M., Carley, J., Gentry, T., Ginder-Vogel, M.A., Fienen, M., Mehlhorn, T., Yan, H., Caroll, S., Pace, M.N., Nyman, J., Luo, J., Gentile, M.E., Fields, M.W., Hickey, R.F., Gu, B., Watson, D., Cirpka, O.A., Zhou, J., Fendorf, S., Kitanidis, P.K., Jardine, P.M., Criddle, C.S., 2006. Pilot-scale in situ bioremedation of uranium in a highly contaminated aquifer. 2. Reduction of U(VI) and geochemical control of U(VI) bioavailability. Environ. Sci. Technol. 40, 3986–3995.
Wu, W.-M., Carley, J., Luo, J., Ginder-Vogel, M.A., Cardenas, E., Leigh, M.B., Hwang, C., Kelly, S.D., Ruan, C., Wu, L., Van Nostrand, J., Gentry, T., Lowe, K., Mehlhorn, T., Carroll, S., Luo, W., Fields, M.W., Gu, B., Watson, D., Kemner, K.M., Marsh, T., Tiedje, J., Zhou, J., Fendorf, S., Kitanidis, P.K., Jardine, P.M., Criddle, C.S., 2007. In situ bioreduction of uranium (VI) to submicromolar levels and reoxidation by dissolved oxygen. Environ. Sci. Technol. 41, 5716–5723.
Wu, W.M., Carley, J., Green, S.J., Luo, J., Kelly, S.D., van Nostrand, J., Lowe, K., Mehlhorn, T., Carroll, S., Boonchayanant, B., Löffler, F.E., Watson, D., Kemner, K.M., Zhou, J., Kitanidis, P.K., Kostka, J.E., Jardine, P.M., Criddle, C.S., 2010. Effects of nitrate on the stability of uranium in a bioreduced region of the subsurface. Environ. Sci. Technol. 44, 5104–5111.
Xie, J.C., Lin, J.F., Zhou, X.H., 2018. pH-dependent microbial reduction of uranium(VI) in carbonate-free: UV-vis, XPS, TEM, and thermodynamic studies. Environ. Sci. Pollut. Res. https://doi.org/10.1007/s11356-018-2326-2.
Xu, A.G., Chao, L., Xiao, H.B., Sui, Y.Y., Liu, J., Xie, Q.J., Yao, S.Z., 2018. Ultrasensitive electrochemical sensing of Hg^{2+} based on thymine-Hg^{2+}-thymine interaction and signal amplification of alkaline phosphatase catalyzed silver deposition. Biosens. Bioelectron. 104, 95–101.
Yong, P., Macaskie, L.E., 1995. Enhancement of uranium bioaccumulation by a *Citrobacter* sp. via enzymically-mediated growth of polycrystalline $NH_4UO_2PO_4$. J. Chem. Technol. Biotechnol. 63, 101–108.
Zhang, J., Song, H., Chen, Z., Liu, S., Wei, Y., Huang, J., Guo, C., Dang, Z., Lin, Z., 2018. Biomineralization mechanism of U(VI) induced by *Bacillus cereus* 12-2: the role of functional groups and enzymes. Chemosphere 206, 682–692.